Journal : Small 11069 Dispatch : 11-11-2011 Pages : 29
Article No. : 9841 ☐ LE ☐ TYPESET
MS Code : ☑ CP ☑ DISK

Nat Hazards
DOI 10.1007/s11069-011-9841-5

ORIGINAL PAPER

An HWRF-based ensemble assessment of the land surface feedback on the post-landfall intensification of Tropical Storm Fay (2008)

Monica Laureano Bozeman · Dev Niyogi · S. Gopalakrishnan · Frank D. Marks Jr. · Xuejin Zhang · Vijay Tallapragada

Received: 31 December 2010 / Accepted: 28 April 2011

Abstract While tropical cyclones (TCs) usually decay after landfall, Tropical Storm Fay (2008) initially developed a storm central eye over South Florida by anomalous intensification overland. Unique to the Florida peninsula are Lake Okeechobee and the Everglades, which may have provided a surface feedback as the TC tracked near these features around the time of peak intensity. Analysis is done with the use of an ensemble model-based approach with the Developmental Testbed Center (DTC) version of the Hurricane WRF (HWRF) model using an outer domain and a storm-centered moving nest with 27- and 9-km grid spacing, respectively. Choice of land surface parameterization and small-scale surface features may influence TC structure, dictate the rate of TC decay, and even the anomalous intensification after landfall in model experiments. Results indicate that the HWRF model track and intensity forecasts are sensitive to three features in the model framework: land surface parameterization, initial boundary conditions, and the choice of planetary boundary layer (PBL) scheme. Land surface parameterizations such as the Geophysical Fluid Dynamics Laboratory (GFDL) Slab and Noah land surface models (LSMs) dominate the changes in storm track, while initial conditions and PBL schemes cause the largest changes in the TC intensity overland. Land surface heterogeneity in

M. Laureano Bozeman (✉) · D. Niyogi (✉)
Department of Earth and Atmospheric Sciences, Purdue University, 550 Stadium Mall Dr., West Lafayette, IN 47907, USA
e-mail: climate@purdue.edu

D. Niyogi
e-mail: dniyogi@purdue.edu

S. Gopalakrishnan · F. D. Marks Jr.
Hurricane Research Division, NOAA/Atlantic Oceanographic and Meteorological Laboratory, Miami, FL, USA

X. Zhang
CIMAS, University of Miami, Miami, FL, USA

V. Tallapragada
NOAA/NWS Environmental Modeling Center, Camp Springs, MD, USA

Florida from removing surface features in model simulations shows a small role in the forecast intensity change with no substantial alterations to TC track.

Keywords Hurricane WRF · Noah · Landfalling tropical cyclones · Post-landfall intensification · Land–atmosphere interactions · Boundary layer processes

1 Introduction

Tropical systems weaken and decay rapidly after making landfall. This decay has been attributed to multiple factors such as change in surface characteristics, latent heat flux source, as well as changes in shear (Tuleya 1994; Kimball 2004). The occurrence of TC strengthening post-landfall is therefore an anomalous feature and is of hydrometeorologic interest to the forecast and disaster response community. Only a few cases of overland storm reintensification have been observed for the Atlantic tropical storms in recent years including TCs Erin (2007), Danny (1997), Fran (1996), and David (1979). Unique to our case study, Tropical Storm Fay (2008) became organized through a first-time intensification overland as opposed to a reintensification as previously mentioned with other notable systems. Interestingly, Fay did not develop a typical TC eye-like structure until after landfall over South Florida (Stuart and Beven 2009). Also of interest is Fay's overland intensification and best track proximity to Lake Okeechobee and the Everglades, which leads to the motivation to study whether the unique Florida surface features may have provided a surface feedback to aid with Fay's intensification overland.

National Hurricane Center (NHC) best track reports that TS Fay made landfall at Cape Romano, Florida at 0845 UTC August 19. Later that day, Fay was observed at its peak intensity of 60 knot maximum winds and a central sea level pressure of 986 mb at 1800 UTC, which occurred near Lake Okeechobee. The eye feature that developed post-landfall was visible in the Melbourne (KMLB) radar imagery from 0929 UTC August 19 until 0212 UTC August 20 (Fig. 1). Fay moved steadily over South Florida and crossed into the Atlantic Ocean at approximately 0600 UTC on August 20, 2008. Therefore, it is hypothesized that the surface features such as the occurrence of the lake and the local landuse heterogeneity may have contributed to the brief but significant overland intensification of TS Fay. We report on the analysis of the changes in TC structure over land using the NHC best track, observations, and Hurricane WRF modeling system (Gopalakrishnan et al. 2010). The HWRF simulations of Fay were conducted from August 19, 2008, 00Z until August 21, 2008, 00Z, with particular focus on the period where the storm center was over the land surface (between August 19, 09Z and August 20, 06Z).

Studies have shown that the underlying surface characteristics such as terrain, land use, soil temperature and moisture, albedo, and surface roughness have great influence on convective systems that pass over areas with surface heterogeneities (e.g., Pielke 2001). In the case of landfalling hurricanes, these systems need to seek energy from the available inland moisture and energy fluxes instead of the ocean, as they continue to dissipate. Due to the shape of Florida's coastline, a number of studies have examined the role of the frequent land and sea breezes on Florida's weather (e.g., Pielke 1974; Wilson and Megenhardt 1997; Baker et al. 2001). Numerical simulations of Florida sea breeze circulation have also shown that due to its large area and circular shape, Lake Okeechobee also causes its own lake breeze circulation (Baker et al. 2001). This lake breeze affects both the weather near the lake causing a cloud-free zone above the lake waters during the

Journal : Small 11069 Dispatch : 11-11-2011 Pages : 29
Article No. : 9841 □ LE □ TYPESET
MS Code : ☑ CP ☑ DISK

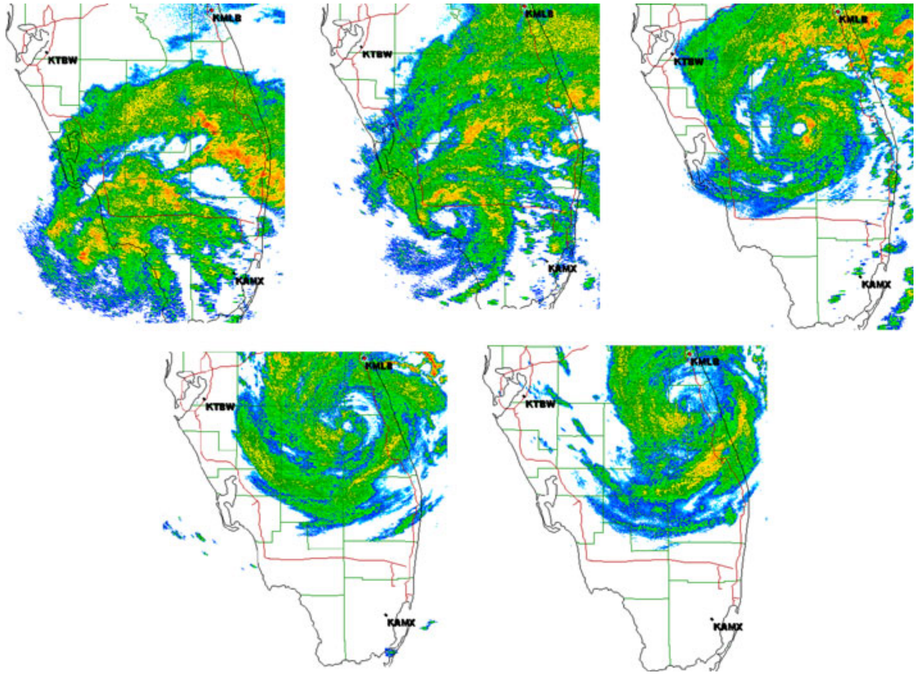

Fig. 1 Melbourne (KMLB) radar images of TS Fay eye development: **a** 0634Z August 19, **b** 0935Z August 19, **c** 1811Z August 19, **d** 0058Z August 20, and **e** 0258Z August 20

day and affects the intensity and duration of the nearby sea breeze circulation occurring on Florida's eastern coastline (Pielke 1974; Boybeyi and Raman 1992).

The overall objective of this study is to understand the impact of the land surface feedbacks on the inland intensification of TS Fay using the HWRF modeling system. The specific goals of our experiments are to: (1) study the effects of different land surface parameterization schemes on the HWRF forecast, (2) study the effect of land surface features (and heterogeneity) including Lake Okeechobee and the Everglades, through idealized simulations, and additionally, (3) assess the relative impact of different ensemble experiments on the model forecast and delineate feedbacks that may have contributed to the post-landfall intensification of Tropical Storm Fay in HWRF simulations.

2 Numerical model and experiments

Model runs were conducted using the HWRF model that implements a stationary parent domain (27 km) and moving inner nest (9 km) and is initialized with the 30-s geography resolution using the WRF preprocessing system (WPS). This configuration of the WRF nonhydrostatic mesoscale model (NMM) core is based on the operational configuration of the NOAA modeling and research centers, in which the different physics options used have been specifically tested for hurricane forecasting and are preferred for predicting TC structure and dynamics (Gopalakrishnan et al. 2010). A detailed description of the HWRF model configurations for our experiments is listed in Table 1; and an in-depth explanation

Journal : Small 11069 | Dispatch : 11-11-2011 | Pages : 29
Article No. : 9841 | ☐ LE | ☐ TYPESET
MS Code : | ☑ CP | ☑ DISK

Table 1 HWRF model configuration for experiments

Domains	
Horizontal	27 km (80° × 80°) *Stationary*
	9 km (6° × 6°) *Moving Nest* (Gopalakrishnan et al. 2010)
Vertical	42 vertical levels with model top at 50 mb
Lateral boundary conditions	6-h GFS forecast on 1° grid
WPS geography resolution	30 s resolution
Model physics	
Number of soil layers	4
Microphysics	Etamp_hwrf scheme (Ferrier 2005)
Long-wave radiation	Modified GFDL scheme (Schwarzkopf and Fels 1991)
Short-wave radiation	Modified GFDL scheme (Lacis and Hansen 1974)
Surface layer	GFDL surface-layer scheme (Moon et al. 2007)
Land surface	GFDL Slab LSM (default)/Noah LSM (Tuleya 1994; Deardorff 1978)/(Ek et al. 2003)
Planetary boundary layer	NCEP GFS Scheme (Hong and Pan 1996)
Cumulus scheme	Simplified Arakawa-Schubert scheme (Hong and Pan 1998)

of the HWRF model domain on a rotated latitude–longitude E-staggered grid is reported in Gopalakrishnan et al. (2011). Since our focus is on TCs over land, the model was initialized only 9 h before landfall, and as a result, we do not use the Princeton Ocean Model (POM) or NCEP coupler components of the operational HWRF. This also helps reduce the degrees of freedom when evaluating Fay's land–atmosphere interactions as opposed to variable sea surface temperatures. In addition, the data needed to initialize the loop current in the POM were unavailable for this case. All simulations are compared with the NHC best track products to assess accuracy in intensity forecasts and with each other to determine the forecast differences between the various alterations of the HWRF model configuration and forecast environment. All results presented in this paper are analyzed from the inner moving nest since it implements a higher model horizontal resolution of 9 km.

Experiments were designed to test the HWRF forecast using two different LSMs: the GFDL Slab model and the Noah land surface model. The GFDL Slab model (Tuleya 1994) uses a bulk subsurface layer to prognostically predict the ground surface temperature assuming the following surface energy balance:

$$
\begin{aligned}
&\sigma {T_L}^4 + H + LE - (S + F\downarrow) = G \\
&H = \rho c_p C_e V (T_L - \theta_{va}) \\
&LE = (WET)\rho L C_e V [R_s(T_L) - R_a]
\end{aligned}
$$

From these energy balance equations, G represents the net ground surface heat flux, H, the surface sensible heat flux, LE is the surface evaporative heat flux, σT_L^4 is the emission from the Earth's surface and finally, $(S + F\downarrow)$ is the net downward radiative surface flux. The drag coefficient C_e is calculated from the Monin-Obukhov methods referenced in Tuleya (1994), where V is the low-level wind speed, θ_{va} is the virtual potential temperature of the surface air. WET represents the wetness coefficient, R_s and R_a are the mixing ratios of the saturated surface land temperature and of the low-level air, L is the latent heat of condensation, ρ is the density of the low-level air, while c_p is the specific heat of air. Once assuming this surface energy balance Tuleya, following Deardorff (1978) predicts the slab model ground surface temperature with the formula below:

$$\frac{\partial T_L}{\partial t} = \frac{-\sigma {T_L}^4 - H - LE + (S + F\downarrow)}{\rho_s c_s d}$$

$$\text{where } d = (\tau\lambda/\rho_s c_s \pi)^{1/2}$$

In the slab surface temperature equation, $\rho_s c_s$ is the soil heat capacity, d is the damping depth where λ is the thermal conductivity of the soil and τ is the period of forcing (24 hours). Since the only predicted variable in the slab model is the surface temperature, all surface fluxes (enthalpy and momentum) are calculated by the surface layer scheme, the surface wetness remains constant with time and is initially specified by the input GFS lateral boundary conditions. During the development of the GFDL hurricane model, the GFDL slab model with conjunction of the GFDL radiation scheme met the requirements for realistic TC activity over land at the time (Gopalakrishnan et al. 2010). Gopalakrishnan et al.'s (2010) tests with HWRF highlight that the simple GFDL Slab model sufficiently replicates important features such as the cold pool land temperature beneath a TC. The

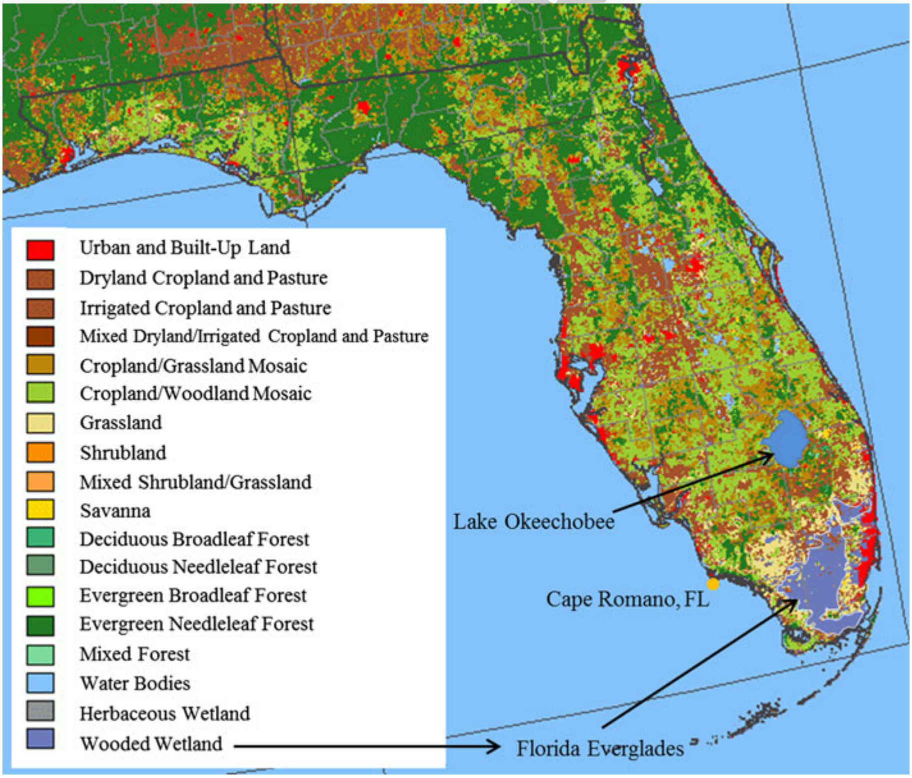

Fig. 2 USGS landuse categories of the dominant 18 landuse categories in Florida produced by the 1 km AVHRR data from April 1992 until March 1993. Image obtained from http://fcit.usf.edu/florida/maps/land_use/land_use.htm and modified to indicate locations of interest

Journal : Small 11069 Dispatch : 11-11-2011 Pages : 29
Article No. : 9841 □ LE □ TYPESET
MS Code : ☑ CP ☑ DISK

simulation of the cold pool is important over land to greatly reduce the surface evaporation and aids rapid TC decay. We hypothesize, however, that the Noah model (Ek et al. 2003) will produce more realistic forecasts due to its implementation of four soil layers and explicit prediction of surface soil temperature, moisture, runoff, sensible heat flux, evaporation, and snow cover. Noah also includes a more complex vegetation representation through the use of the USGS 1992 and MODIS 2001 land use datasets. In this study, the Slab model runs are the control because current operational hurricane models (i.e., GFDL hurricane model and HWRF) employ the GFDL Slab model as the default LSM, while numerous operational NCEP models use the Noah LSM, which we will use as the experimental LSM.

To study the impact of the unique Florida surface features, the USGS landuse and soil type (top and bottom soil type) of the 30-s resolution geography tiles were altered to reflect the "removal" of Lake Okeechobee and the Everglades in experimental runs (locations of these features are indicated in Fig. 2). Landuse and soil type categories were changed to values similar to each feature's surroundings as per the default USGS 1992 dataset (Fig. 2) to avoid creating artificial heterogeneous land and soil surfaces. Removal of Lake Okeechobee/Everglades is reflected by changing the 24 category USGS landuse category, 16 category soil type—top and bottom from water/wooded wetland to dry cropland and pasture/grassland, sand/sand, and sand/bedrock, respectfully. The model land/sea mask is then calculated by the model and is determined from the landuse category as either water or land. Changes were done to the soil and landuse to dry out the land surface that the TC will pass over to investigate the impacts on the surface environment and TC rainfall distribution and structure. The relative influence of each surface feature is evaluated by a variable isolation analysis through model experiments (Table 2). Experiments were conducted with both Lake Okeechobee and the Everglades removed (NOWET), and additional model runs to separately test the contribution of (a) only Lake Okeechobee removed (NOLAKE) and (b) only the Everglades removed (NOGLADES), to determine the relative impact of each wet area on the moisture and temperature distribution of tropical storm Fay.

Sections 3 and 6 of this paper discuss the results of the model simulations and conclusions, respectfully. The organization of the subsections of Sect. 3 is as follows: a description of the results from the control and default LSMs is in Sect. 3.1, simulations specific to Lake Okeechobee and the Everglades in Sect. 3.3, and an assessment of the improved results seen with the use of the Noah LSM, a Noah-based HWRF ensemble is analyzed in Sect. 3.4. In Sects. 3.2 and 3.5, we revisit the Noah LSM intensity analysis and then proceed to take a more in-depth analysis of possible influences of storm decay. The storm decay discussion involves simulations implementing real-world (i.e. default)

Table 2 LSM model runs with changed surface features

Run name	LSM used	Experimental change
Slab (S)	GFDL Slab LSM	
NOWET (SW)	GFDL Slab LSM	Lake and Everglades removed
NOLAKE (SL)	GFDL Slab LSM	Lake Okeechobee removed only
NOGLADES (SG)	GFDL Slab LSM	Everglades removed only
Noah (N)	Noah LSM	
NOWET (NW)	Noah LSM	Lake and Everglades removed
NOLAKE (NL)	Noah LSM	Lake Okeechobee removed only
NOGLADES (NG)	Noah LSM	Everglades removed only

geography, all-ocean over the region of Florida, and finally no ocean surrounding Florida while Lake Okeechobee and the Everglades are still present in the idealized geography from the WRF Preprocessing System (WPS). In Sect. 3.5, a simplistic water budget is analyzed from the model simulations used in Sect. 3.2. Since forecast skill is largely assessed based on forecast track, each subsequent section of the results and discussion begins with an analysis of the forecast track error, referred to here as FTE. In TC prediction, FTE is defined as the great circle distance of the forecast latitude (lat$F$) and longitude (lon$F$) points from the observed best track latitude (lat$B$) and longitude (lon$B$) points over the globe. This is calculated from Powell and Aberson (2001):

$$\mathrm{FTE} = 111.11 * \arccos[\sin(\mathrm{lat}B) * \sin(\mathrm{lat}F) + \cos(\mathrm{lat}B) * \cos(\mathrm{lat}F) * \cos(\mathrm{lon}B - \mathrm{lon}F)]$$

Next, TC intensity forecasts are of importance to assess the internal storm dynamics and also to investigate the causes of periods of storm strengthening and weakening. These results are discussed in the Sect. 3.1.2. Section 3.1.2 analyzes the intensity forecasts for simulations using the GFDL Slab and Noah LSM, and then proceeds to take a more in-depth analysis of possible influences of storm decay. The storm decay discussion involves simulations implementing real-world (i.e., default) geography, all-ocean over the region of Florida, and finally no ocean surrounding Florida, while Lake Okeechobee and the Everglades are still present in the idealized geography from the WRF preprocessing system (WPS). Section 3.3.2 analyzes the model intensity forecasts focused on the effects of the presence of Lake Okeechobee and the Everglades and uses results of the no ocean simulation to supplement the discussion (Sect. 3.3.4), while Sect. 3.4.2 investigates intensity forecasts from the findings in the Noah-based ensemble. Subsequent Sect. 3.4.3 involve investigation of the model-simulated rainfall accumulations.

3 Results and discussion

3.1 Influence of GFDL Slab versus Noah LSM

3.1.1 Forecast track errors

Figure 3a shows the 6-h FTE (km) between model runs using the GFDL Slab and Noah LSM against the best track. Our focus is on the track error columns corresponding to "S" and "N" at this time. Both Slab and Noah deviate from the best track over the ocean from the initial time, but in the first 6 h, Noah and Slab have a similar forecast track, and then begin to separate from each other after this time. The Noah run begins to realign itself by intersecting the best track near the time of the observed landfall at Cape Romano, while Slab places the landfall location further west. Overall, the Noah run stays fairly consistent to the best track forecast, but with a slight 6 h position lag resulting in a lower sum of 6-h forecast errors (sum FTE) of 78.39 km. The Slab model keeps the storm following Florida's western coastline and farther into northern Florida resulting in a very large total FTE of 401.37 km.

3.1.2 Intensity errors

Figure 4a shows the maximum sustained winds along the forecast track for Slab versus Noah. From the time series, both Slab and Noah correctly categorize Fay's TS intensity; however, both LSM runs underestimate the observed peak winds of 60 knots at 18Z on

Journal : Small 11069 Dispatch : 11-11-2011 Pages : 29
Article No. : 9841 ☐ LE ☐ TYPESET
MS Code : ☑ CP ☑ DISK

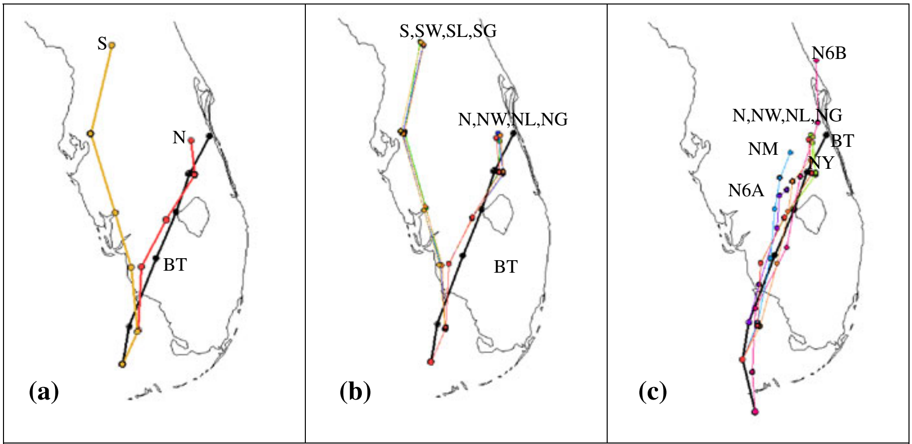

		GFDL SLAB LSM				NOAH LSM							
Time	**fcst hr**	**S**	**SW**	**SL**	**SG**	**N**	**NW**	**NL**	**NG**	**NY**	**NM**	**N6B**	**N6A**
08/18 18Z	-6											0	
08/19 00Z	0	0	0	0	0	0	0	0	0	0	0	25.09	
08/19 06Z	6	14.80	15.46	14.91	15.42	15.24	15.50	15.33	15.40	18.77	13.92	23.26	0
08/19 12Z	12	19.68	18.92	19.23	19.19	14.79	14.40	14.20	14.95	12.46	5.32	12.39	45.35
08/19 18Z	18	28.11	29.92	28.32	28.65	11.96	13.59	12.47	12.85	4.05	9.92	49.25	27.28
08/20 00Z	24	147.56	140.46	143.34	141.81	6.37	10.83	11.41	5.19	21.53	33.08	75.29	44.58
08/20 06Z	30	191.24	187.58	187.32	192.33	30.03	22.02	25.68	25.66	44.87	62.52	111.63	96.32
Sum FTE		**401.37**	**392.35**	**393.12**	**397.40**	**78.39**	**76.34**	**79.10**	**74.05**	**101.68**	**124.77**	**296.91**	**213.53**

Fig. 3 HWRF model forecast track errors (FTE): **a** GFDL Slab versus Noah, **b** GFDL Slab land changes (SW, SL, SG) versus Noah LSM land changes (NW, NL, NG), **c** Noah LSM ensemble members (NW, NL, NG, NY, NM, N6B, N6A). Fay best track (BT) forecast is indicated with the *thick black line*

August 19. Once over land, Slab shows a dramatic reduction in wind speed especially from 18Z August 19 until 03Z August 20. Noah was able to correctly predict the secondary peak winds of 55 knots at 12Z August 19 and at 00Z August 20, but these winds weakened quickly after 00Z, and thus under predicting the 50 kt observation at 06Z August 20. Figure 5a shows the along-track minimum sea level pressure (MSLP) over time for Slab versus Noah. From the initial time, both LSMs drop the central pressure drastically for the brief period over the ocean, then show slow storm filling after landfall. Both Slab and Noah keep the central pressure of Fay too deep during the time of the observed minimum pressure of 986 mb and instead simulate 984.8 and 983.6 mb, respectively. The runs only show a moderate weakening of Fay after 18Z August 19, while Slab shows a secondary strengthening starting at 22Z on August 19.

3.2 Revisiting the Noah LSM Intensity Analysis and Mechanisms for Decay

Since the Slab LSM was unable to produce an adequate track forecast, a generalized analysis of TS Fay decay mechanisms will only include model simulations using the Noah LSM. Figure 13 shows different parameters for decay of the Noah default simulation

Journal : Small 11069 Dispatch : 11-11-2011 Pages : 29
Article No. : 9841 □ LE □ TYPESET
MS Code : ☑ CP ☑ DISK

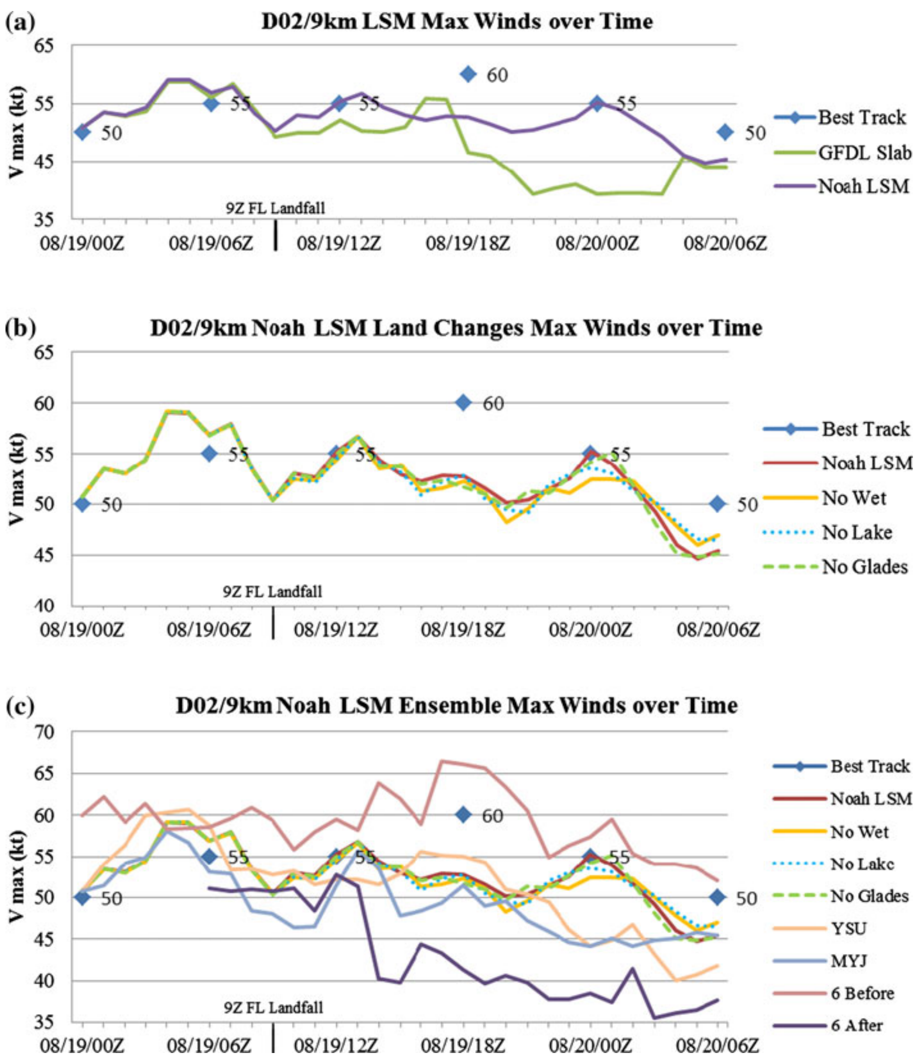

Fig. 4 Along-track maximum winds (kt) for 00Z August 19 until 06Z August 20: **a** GFDL Slab versus Noah LSM, **b** Noah LSM land changes, and **c** Noah LSM ensemble. Fay's Florida landfall on Cape Romano at 09Z on August 19, 2008, is indicated by the *black line*

versus the Noah-based ALLOCEAN and NOOCEAN idealized simulations. By including nonlandfall simulations with ALLOCEAN and NOOCEAN, we can investigate the role of oceanic sustenance of the TC, if Florida were not present, and the rapid decay of the TC from being initialized and traversing over a nonmoist region for an extended period of time (in addition to the roughness and friction characteristics of the land surface). In addition, the storm structure due to the transition of the TC from water to land can be compared in the default Noah run compared with the nonlandfalling simulations. The predicted storm tracks of the ocean test simulations (not shown) have Fay tracking similarly to the best track and Noah default in the ALLOCEAN run and more to the west (similar to the Slab

Journal : Small 11069 | Dispatch : 11-11-2011 | Pages : 29
Article No. : 9841 | ☐ LE | ☐ TYPESET
MS Code : | ☑ CP | ☑ DISK

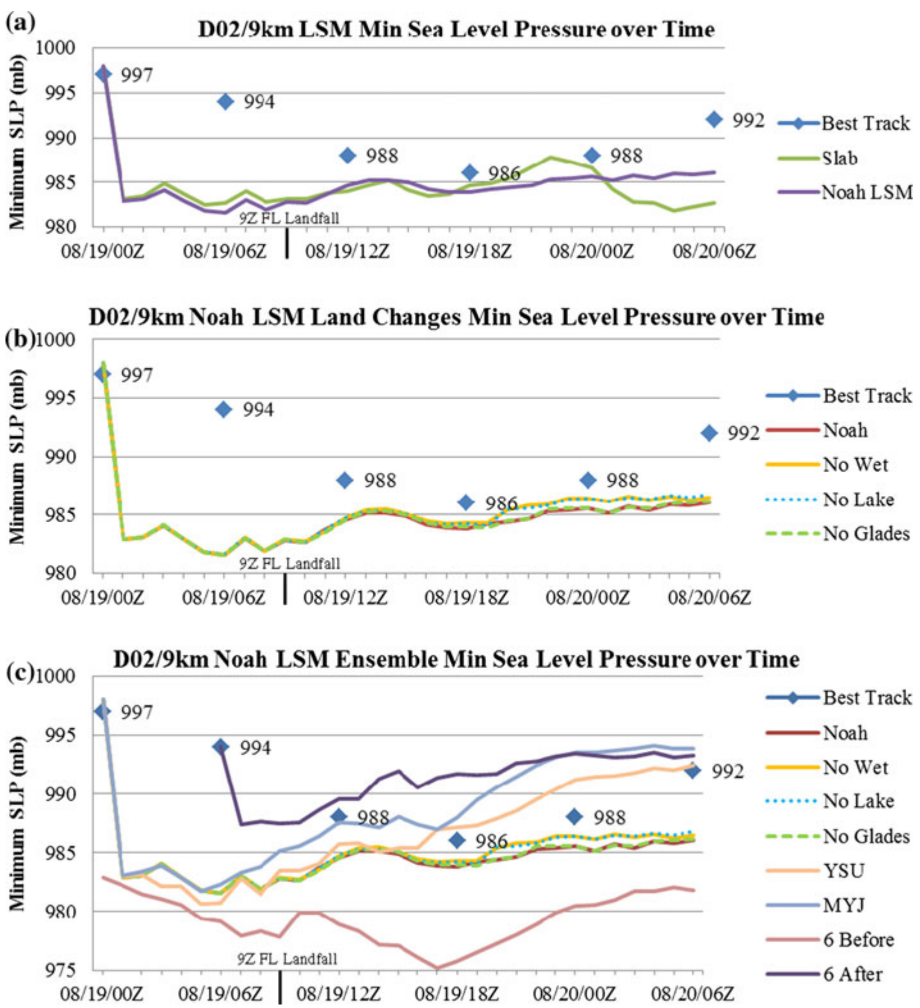

Fig. 5 Same as Fig. 4 but for mean sea level pressure (mb, MSLP)

track) with the NOOCEAN run (NOOCEAN track is seen and discussed later in Fig. 11). Figure 13a shows the simulated MSLPs compared with the 6-h best track MSLP. The default Noah simulation is the most comparable to the best track, while the ALLOCEAN and NOOCEAN are the upper and lower bounds on the central pressure, respectively. These results agree with the past studies of landfalling TCs that are not able to maintain strength over land. Figure 13b shows the maximum sustained winds at 10 m compared with the NHC best track storm sustained winds. The 10-m Vmax is displayed since it takes into account the local exposure to the surface roughness from the land surface model. However, the maximum sustained winds in the storm (i.e., “storm Vmax”) (not shown for ALLOCEAN and NOOCEAN, while the Noah default Vmax is seen in Fig. 4a) are more comparable to the NHC Vmax since they do not address the local roughness and are better representative of open-terrain exposure. As such, the values of the 10-m Vmax are lower and probably more in agreement with local station observations that were not studied in this paper. In Fig. 13b, NOOCEAN shows a rapid decay of winds, while ALLOCEAN reveals extremely strong winds despite being restricted to the 10 m level. In a simplistic view, these two plots indicate that TCs intercepting and/or traversing overland does in fact drastically reduce storm strength when compared with an all water case.

TC decay post-landfall is attributed to numerous factors based on the land surface characteristics, yet the greatest of these is the reduction in latent heat energy and evaporation once over land (Tuleya and Kurihara 1978). Surface latent and sensible heat fluxes, frictional stresses, and roughness are important variables for TC maintenance over land and therefore are reviewed to see how the predicted TC intensity may have been affected by these parameters (Tuleya and Kurihara 1978; Dastoor and Krishnamurti 1991; Shen et al. 2002). Figure 13c–e show the storm tangential latent heat flux, sensible heat flux, and frictional stress (with zero value fluxes removed) to help assess factors contributing in the rates of strengthening and decay observed in these simulations. For the latent heat flux field (Fig. 13c), the Noah default curve is as expected with higher latent heat over ocean and then a significant reduction in latent heat similar NOOCEAN curve post-landfall. Since Lake Okeechobee is still present in the NOOCEAN case, it is interesting to find that this latent heat curve shows a slight increase between 12Z and 18Z on August 19th when the TC track nears the lake. After the slight increase in the latent heat flux, the NOOCEAN tangential flux tapers off near the end of the time series and never returns back to the low initial latent heat values as in the beginning of the forecast period before the lake moisture source was introduced. The ALLOCEAN latent heat curve, however, shows a more dramatic flux increase near 18Z. Since latent heat performs as expected when the system transitions from ocean to land, it is possible that the sensible heat flux may play a more dominant role in maintenance or decay in the case of TS Fay. Figure 13d shows the sensible heat flux for each of the ocean test cases, and again, the ALLOCEAN and NOOCEAN are the upper and lower bounds of the flux over time. While one would think that the Noah default case should act similarly to the NOOCEAN case overland, we must highlight that the Florida peninsula is a landmass with a small width compared with the scale of the storm. So as TS Fay passes over the Florida landscape, it is still being influenced by the surrounding sea. As the storm crosses over the Florida peninsula, the rainbands swirling over the ocean are still impacting the energy transfer within the core either by slowing the amount of evaporation or through advection of moisture inwards. Evidence of this can be seen by the fact that the Noah default sensible heat does not drop down as far as the NOOCEAN sensible heat curve despite being over land. Horizontal flux gradients between the peninsula land and surrounding sea are smeared by the horizontal advection as the storm rainbands swirl over both land and sea. Tangential frictional stress over time (Fig. 13e) suggests that for a water case, as in ALLOCEAN, the stronger the wind, the stronger the frictional stress becomes over time. However, for a land case, the evolution of the frictional stress is more complicated. As seen in NOOCEAN, there is an initial increase in stress yet as the wind spins down due to interactions with the land surface, the net stress decreases more rapidly in model simulations over land. Further evidence of both of these trends can be seen in the Noah default curve for frictional stress, where just after landfall there is a brief peak in stress similar to the NOOCEAN case. Then, once the Noah default storm nears Lake Okeechobee, another peak in stress develops (similar to the ALLOCEAN case) since the wind field may have become stronger from traversing over a water body with less surface roughness (Shen et al. 2002).

Journal : Small 11069 Dispatch : 11-11-2011 Pages : 29
Article No. : 9841 LE TYPESET
MS Code : CP DISK

3.3 Influence of Lake Okeechobee and Florida Everglades

3.3.1 Forecast track error

Figure 3b shows results for the 6-h FTE for the Slab and Noah simulations involving land surface feature changes in the presence or lack of Lake Okeechobee and the Everglades. We focus on the track error table of both columns of "NW", "NL", and "NG" corresponding to "SLAB" and "NOAH". Every land change model run follows their parent LSM run well; however, the tracks of the land changes for the Slab model have more variance between each 6 h position. Slab shows 6 h position variation from forecast hours 12–30, whereas the Noah runs show position variation from the parent LSM for forecast hours 24–30. Interestingly, the different land changes for the Slab model have lower total FTEs than the Slab run itself. The land changes with Noah have lower total FTEs with the exception of the NL run, which has a higher total FTE from Noah by 0.71 km. The lowest FTEs for all Noah runs occurred at forecast hours 18–24, while FTE for all Slab runs steadily increased over time as the storm was incorrectly moving westward.

3.3.2 Intensity error

Figures 4b and 5b show time series of the along-track maximum sustained winds and MSLP for the land change runs with the Noah LSM only. These time series are only for the Noah runs since the Noah track brought the storm closer to the surface features being studied. Figure 4b shows that the runs follow the original Noah wind time series fairly closely over time and continue to classify Fay with TS strength. All wind curves agree over water, but after landfall, the curves begin to deviate slightly from each other. A similar pattern to the storm maximum winds can be seen in the 10-m sustained winds over time (not shown). On average, the Noah run maintains the highest winds and usually is the upper bounding curve, while the NW run is the lower bound in this time series. As Fay nears Florida's eastern coastline, the wind speeds of the NL and NW runs increase and have a higher magnitude than the Noah and NG runs beginning at 02Z August 20th. Differences between the wind speeds at 06Z August 20 are small, 1–1.5 knot differences. Figure 6 shows the spatial plots of the wind differences. In any run where the lake is removed reveals a large under prediction of the 10 m wind by as much as 10–30 knots. In cases where the Everglades are taken out, the differences are typically ±5 knots, with the location of the differences varying from run to run. Figure 5b shows that the land changes do have a small influence on the TC central pressure. Shortly after landfall, the MSLP curves deviate from each other, with the largest pressure differences after the observed peak intensity. The NL and NW runs predict Fay to weaken faster after passing the peak time, as the Noah and NG runs show a slow steady weakening until 06Z August 20. These plots indicate that the presence of Lake Okeechobee caused slight but detectable enhancement of the storm central pressure and wind speed as the TC crosses near and over the lake; the contribution of the possible lake feedback will be discussed in the next section.

A cross-sectional analysis (see Figs. 7, 8) was completed to view additional differences in surface variables along the land and directly above the lake at the time of Fay's peak intensity. The cross-section was taken at constant latitude of 26.95°N across Florida and Lake Okeechobee with longitude varying from −82.1°W to −80.1°W. The cross-section lines in the Slab runs are shifted slightly due to the variation in forecast track between land change runs that were more pronounced in Slab simulations. The cross-section analysis

Journal : **Small 11069** Dispatch : **11-11-2011** Pages : **29**
Article No. : **9841** ☐ LE ☐ TYPESET
MS Code : ☑ CP ☑ DISK

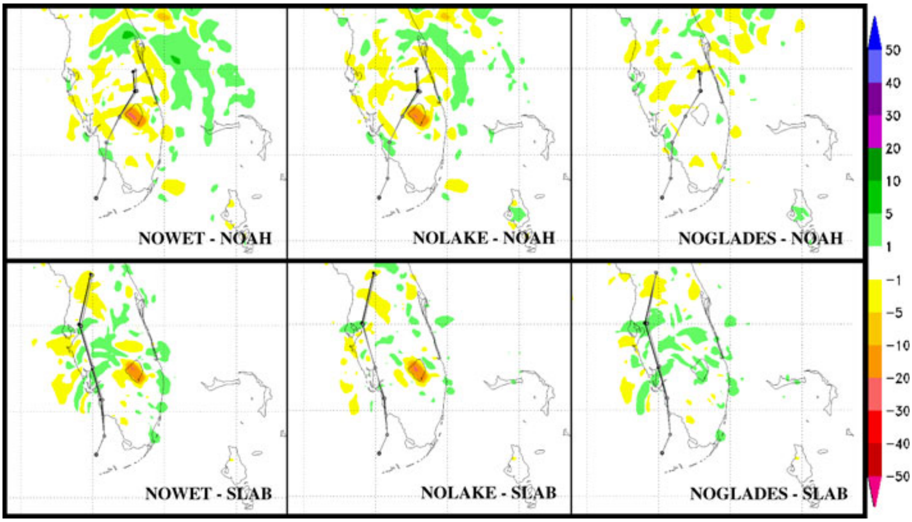

Fig. 6 Noah (*top*) and GFDL Slab (*bottom*) LSM land changes 10-m wind differences (kt) from 00Z August 19 until 06Z August 20

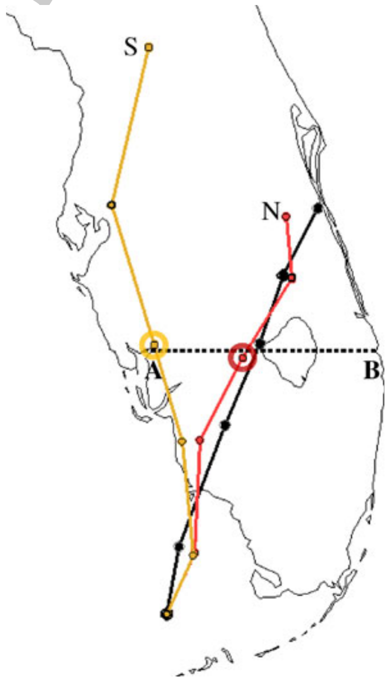

Fig. 7 *Dotted line* (*A*–*B*) indicates the location of the cross-section for the GFDL Slab (S) and Noah (N) LSM tracks. The *large circles* along each track indicate the position of the storm at the time of the cross-section images (18Z August 19)

reveals that for both Noah and Slab, when the lake is present, there are increased surface latent heat fluxes and 10 m wind speeds directly over the lake. This is consistent with the increased humidity and decreased roughness of the water surface. Both the LSMs predict a lower central pressure than observed by the best track, yet Slab has a weaker central

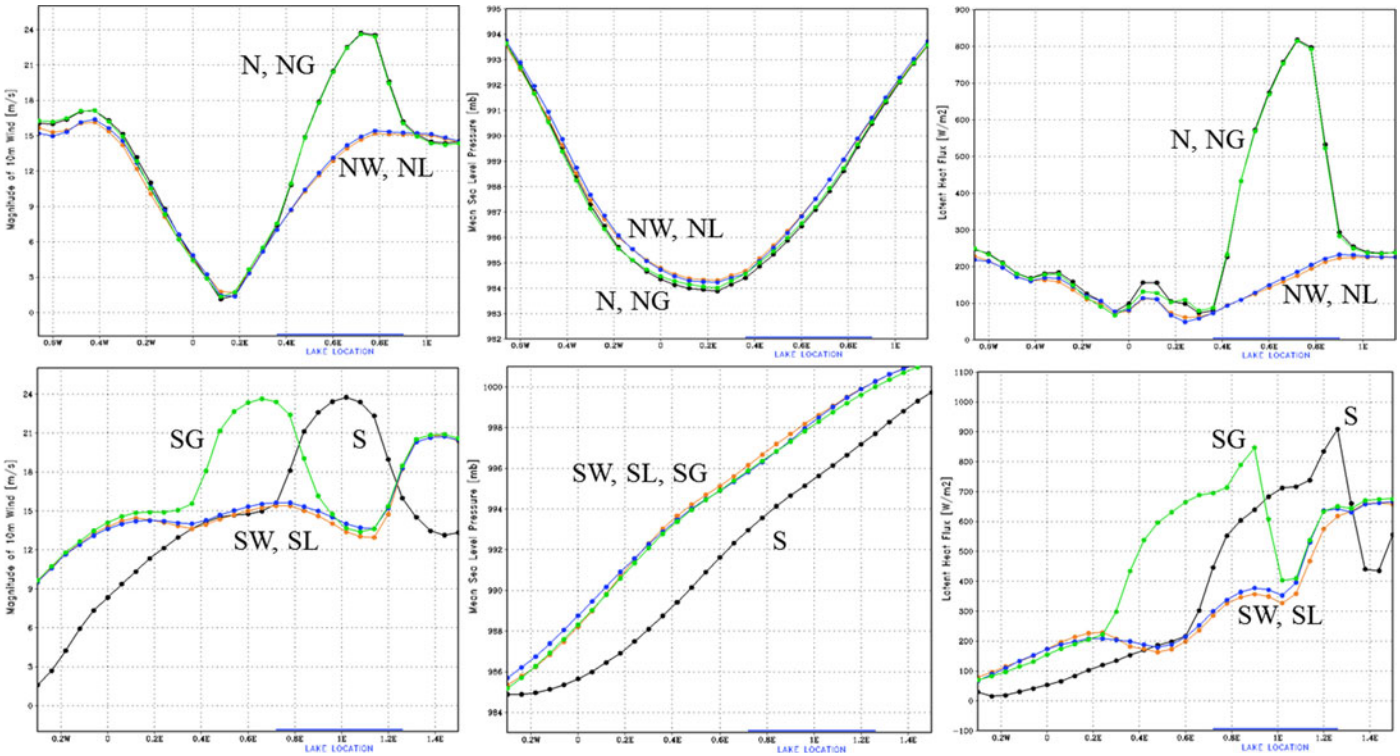

Fig. 8 Noah (*top*) and GFDL Slab (*bottom*) LSM land changes horizontal cross-section plots for the magnitude of the 10 m winds (*left*), MSLP (*middle*), and surface latent heat flux (*right*) at 18Z August 19, along the cross-section line **a**–**b** shown in Fig. 7

Journal : Small 11069 Dispatch : 11-11-2011 Pages : 29
Article No. : 9841 ☐ LE ☐ TYPESET
MS Code : ☑ CP ☑ DISK

pressure than Noah by about 1 mb. Consistent with the intensity analysis, runs without Lake Okeechobee have a weaker central pressure, though the SG curve follows the SL and SW curves as opposed to being similar to the Slab parent run. A study by Sousounis and Fritsch (1994) shows that lakes may enhance precipitation in strong synoptic systems, but will not alter storm tracks. Their study conducted for the Great Lakes suggests that lakes may help storms intensify and cause a 3–4 mb drop in MSLP for strong synoptic extra-tropical cyclones passing over the lake region. Shen et al. (2002) studied the simulated rate of decay on landfalling TCs using the GFDL hurricane model when standing surface water of various depths was present over the land surface. They concluded that a half meter of standing surface water was able to reduce the rate of TC decay after landfall. In our model study, though, the pressure is not lowered to the same degree as the effect of the Great Lakes on extratropical systems.

3.3.3 Surface heterogeneity effects on rainfall accumulations

The simulation of TC rainfall magnitude and spatial coverage was also dependent on the choice of the land surface scheme, in part due to the forecast track. Figure 9 shows the differences in rainfall accumulation from the default LSM runs for the land surface changes described in Table 3. In particular, the spatial coverage of the rainfall maxima covers a broader area in the Noah run, while the Slab-based maxima is placed farther north with a greater magnitude by 100 mm. Overall, the TC rainband circulation is more coherent in the difference plots than with the Slab LSM. In all runs, there is an expected eastward precipitation bias that is consistent with the observations that the maximum rain fall occurs within the right-front quadrant of the system as it moves forward in time (Marchok et al. 2007). The most impact to the rain field can be seen with each NW run and is mainly due to the elimination of Lake Okeechobee. There are small but noticeable differences between rain accumulations when the lake is not present resulting in an under prediction of nearly 10–20 mm for most runs and up to 20–30 mm in the case of NW and SL runs. For this case, the Everglades has a minimal impact on rainfall accumulation, though its elimination did affect the magnitude by over predicting rainfall near the Everglades and the Florida Keys in the Slab LSM runs. Interestingly, the presence of the lake also prevents an over prediction of rainfall directly of the south east coast of Florida shown in the NG run. As seen in Fig. 9, the land surface physics choice and land surface heterogeneity cause detectable impacts on the TC rainfall distribution.

3.3.4 TC development solely influenced by land surface moisture sources

To further isolate the possible influence of Lake Okeechobee and the Florida Everglades on Fay, the ensemble runs were compared with a simulation with both the Gulf of Mexico and the Atlantic Ocean moisture sources removed (ALLOCEAN or NOOCEAN). In this simulation, the removal of these ocean basins is reflected by changing the 24 category USGS landuse category, 16 category soil type—top and bottom from water to cropland and woodland mosaic, sand, and sand, respectfully, while the original values of the lake and the Everglades remained unchanged. The goal of this model run is to eliminate the TC spiral rainbands from obtaining moisture from the ocean basins as the storm center is influenced by land. Instead, this forces Fay to take in moisture from the only available sources—Lake Okeechobee and the Florida Everglades. We hope that including this simulation will isolate and further help to reveal the influence specifically from these features.

Journal : **Small 11069** | Dispatch : **11-11-2011** | Pages : **29**
Article No. : **9841** | ☐ LE | ☐ TYPESET
MS Code : | ☑ CP | ☑ DISK

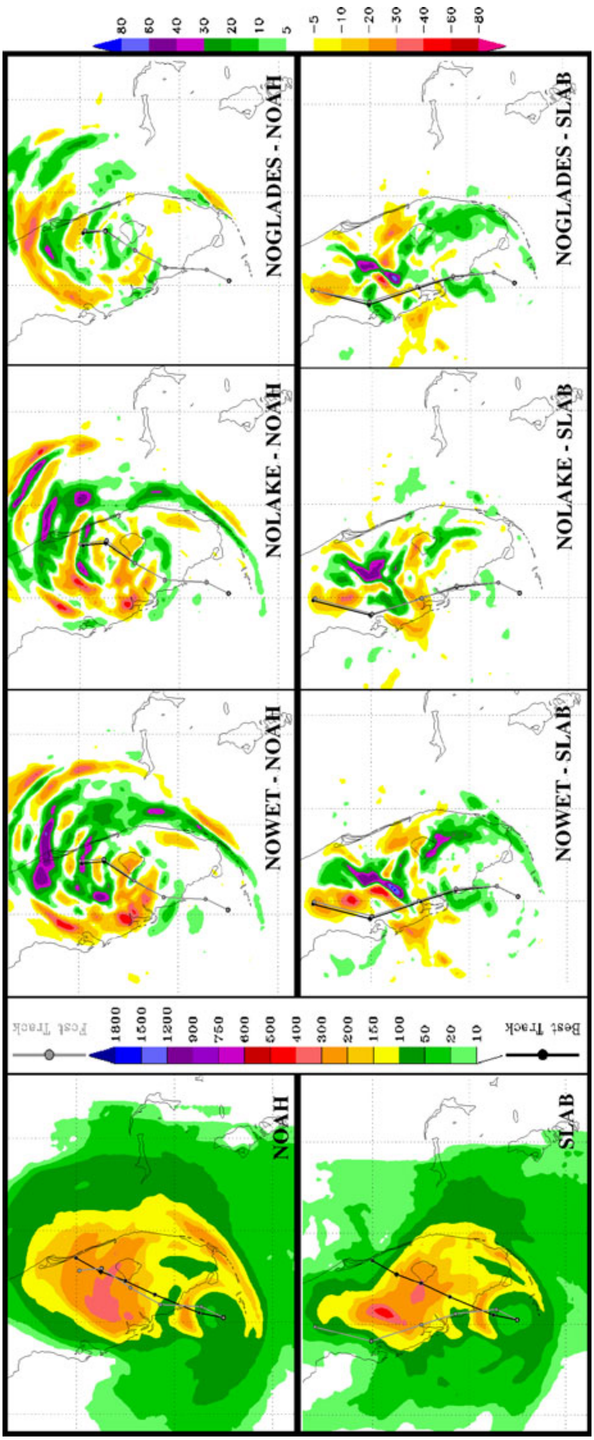

Fig. 9 *Far Left* Noah (*top*) and GFDL Slab (*bottom*) LSM accumulated rainfall (mm) from 00Z August 19 until 06Z August 20. *Right* Accumulated rainfall differences for land surface changes for the same time period

Journal : Small 11069 | Dispatch : 11-11-2011 | Pages : 29
Article No. : 9841 | ☐ LE | ☐ TYPESET
MS Code : | ☑ CP | ☑ DISK

Table 3 Noah LSM ensemble members

Member name	LSM used	Experimental change
Noah (N)	Noah LSM	
NOWET (NW)	Noah LSM	Lake and Everglades removed
NOLAKE (NL)	Noah LSM	Lake Okeechobee removed only
NOGLADES (NG)	Noah LSM	Everglades removed only
YSU PBL (NY)	Noah LSM	YSU PBL scheme
MYJ PBL (NM)	Noah LSM	MYJ PBL scheme
6 Before (N6B)	Noah LSM	Model start time: 2008-08-18 18 Z
6 After (N6A)	Noah LSM	Model start time: 2008-08-19 06 Z

Figure 10 shows the forecast track of the NOOCEAN run compared with the NHC best track (left) and the default Noah track (right). NOOCEAN tracks similarly to the best track and the default Noah from the initialization time through forecast hour 12, then the track brings Fay westward from the best track through the middle of the Florida peninsula, however, not as far west as the Slab run. This forecast track results in a total FTE of 647 km error. A time series of the NOOCEAN maximum winds and MSLP (not shown) reveals a TC of a much weaker intensity with a peak wind of 51.7 kt at 12Z August 19 followed by a steady decrease in wind speed. For the MSLP, there is an initial drastic drop in pressure to 984.2 mb followed by a rapid filling of the central pressure up to 1,001.14 mb at 06Z on August 20th.

Now that they are not being overpowered by the influence of the ocean water, Figs. 10 and 11 help to describe the specific contributions of the Florida surface features to the TC structure. Referring back to Fig. 10, the rainfall has accumulated in a diagonal swath across Florida and encompassing Lake Okeechobee. The difference plot of the accumulated rainfall (Fig. 10) shows that the total rain field has been reduced since the NOOCEAN simulation is a weaker storm in a drier environment, yet has a grossly overpredicted rain swath as compared to the defaultNoah run probably due to the fact that the Everglades and Lake Okeechobee were the only sources of moisture. Perhaps the moist surface features

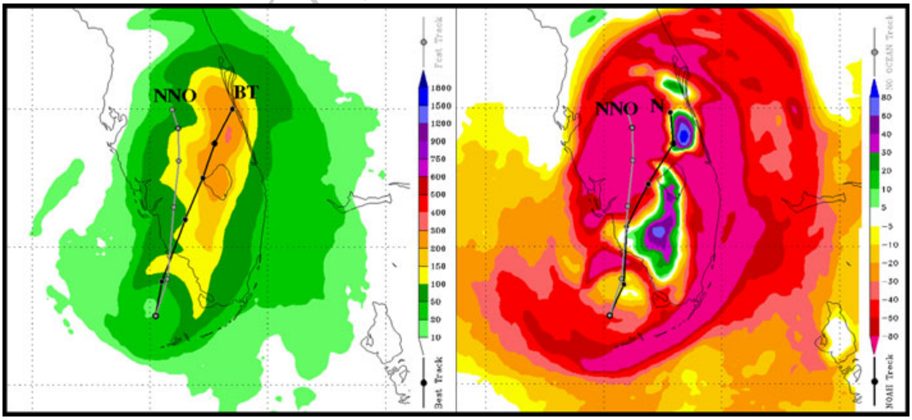

Fig. 10 *Left* Noah No Ocean (NNO) forecast track and accumulated rainfall (mm). *Right* No Ocean rainfall accumulation and track difference from the Noah default (N)

Journal : Small 11069 Dispatch : 11-11-2011 Pages : 29
Article No. : 9841 LE TYPESET
MS Code : CP DISK

allowed for enhanced precipitation in the region near Lake Okeechobee that could possibly lead to a surface feedback between the falling precipitation and the accumulating soil moisture over a larger area. This feedback follows the study of Emmanuel et al. (2008) for the warm-core cyclone rainfall in Northern Australia and Chang et al. (2009) for the Indian monsoon region. In Fig. 11, the difference in the 10 m wind reveals that since the lake is a water body with low roughness length, the NOOCEAN wind field is highest surrounding the lake which agrees with Kimball (2004). The high winds over the lake found in the NOOCEAN run may also suggest that in the model simulation, Lake Okeechobee does create its own circulation (Boybeyi and Raman 1992).

3.4 Noah ensemble runs

To further analyze the improvements in the storm simulation using the Noah LSM, we conducted a Noah-based model ensemble assessment with changes to the PBL parameterization, and the initial conditions (Table 3).

3.4.1 Forecast track errors

Referring to Fig. 3c for the 6-h forecast track error between ensemble model runs using the Noah LSM for simulations involving changes to the land surface features, PBL parameterization, and model initial conditions. Interestingly, all of the new ensemble members have higher total FTEs than Noah and the land change runs of which, both the initial condition runs have the highest track error. The N6B run has a large FTE of 296.91 km as it moved the storm too quickly through Florida for all hours except during the first 6 h into

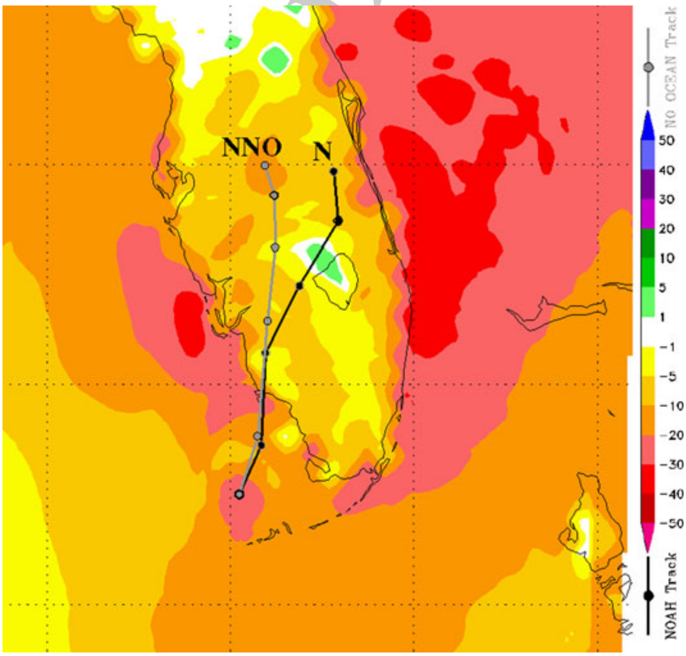

Fig. 11 Noah No Ocean (NNO) difference in 10 m wind magnitude from the Noah default (N)

Journal : Small 11069 Dispatch : 11-11-2011 Pages : 29
Article No. : 9841 □ LE □ TYPESET
MS Code : ✔ CP ✔ DISK

the forecast. Also the N6B run puts Fay at the Atlantic coast at 00Z August 20 and then alters the track northward and into the Atlantic before 06Z August 20, no other run exhibits this behavior. Despite having fewer hours of error to sum up, the N6A run also has a large FTE of 213.53 km since the track stops short as the storm weakens never reaching the Florida's eastern coastline. The NY and NM runs also end their tracks in the middle of Florida as well, but do not have nearly as large error as the N6A run. These systems that dissipate over Florida would have a large intensity error that is discussed later. With exception of the NY run at 06Z August 19, the PBL change runs have a lower six hourly track error than Noah and all the land change runs for 06Z August 19 until 18Z August 19, with the least error at 18Z. Thus, the effect of the land surface feedbacks affecting the TCs is through the boundary layer forcing.

3.4.2 Intensity error

Figures 4c and 5c show time series of the along-track maximum sustained winds and MSLP for the Noah LSM ensemble. In contrast to the Noah land changes, each new member wind field (Fig. 4c) varies dramatically from each other from the initial time until the end of the period of interest and is not able to match the best track winds for any forecast hour. On average, the N6B run maintains the highest winds and usually is the upper bounding curve, while the N6A run is the lower bound in the time series. The N6B run does not match the best track wind observation at 00Z August 19 since this model was initialized 6 h prior and has already deviated from the best track winds. This is not the case for most of the other members that were initialized at 00Z and therefore correspond to the best track at this time. Even though the N6A run was initialized at 06Z August 19, it under predicts the maximum winds to 51.1 kt instead of matching the best track value of 55 kt winds. While all other members are unable to predict a TC with the correct wind intensity at 18Z August 19, the N6B run actually predicts a much stronger TC with peak winds of 66.1 kt, a weak category 1 hurricane. Both the changed PBL runs (MYJ and YSU) start out with strong winds over ocean, then reduce the wind speed post-landfall, and still miss the observed peak wind at 18Z. For most forecast times, the NY run has stronger winds than the NM until 00Z August 20 when the NY weakens the winds quickly, while the NM curve begins to flatten out through 06Z August 20. From this time series, one can see that the only members that match the best track winds most consistently are the default HWRF configuration with Noah, and Noah land change runs each implementing the GFS PBL scheme and initialized at 00Z August 19.

Figure 5c shows that changes in the PBL scheme and initial conditions also have a dominant effect on Fay's along-track MSLP over time for all the Noah ensemble members. Again, the N6B and N6A runs are the outer bounds for the stronger and weaker central pressure intensity, respectively. Changing the PBL parameterization resulted in weaker TCs. The Noah and the land change runs simulate a stronger central pressure at the time of peak intensity, while the PBL changes result in a weaker central pressure for all hours after landfall as compared with the land change runs. This finding is consistent with Gopalakrishnan et al. (2010) who also found that HWRF runs with the MYJ PBL and surface layer parameterization schemes caused weaker TCs. On average, the NY member is the closest to accurately predicting Fay's central pressure. Despite predicting a slightly weaker central pressure during the peak time, NY displays the weakening after 18Z to a more realistic degree than any other ensemble member. NM, however, weakens the TC too quickly after the time of peak intensity, while the land changes cause little variability and continue to maintain the TC strength as it nears Florida's eastern coast.

3.4.3 PBL and initial condition effects on rainfall accumulations

The effect of changes in the model physics and initial conditions on the TC intensity forecast additionally alters the TC rainfall accumulations (Fig. 12). As expected, due to the N6A model producing an extremely weak TC, the rain shield is also severely weakened in both breadth of spatial coverage and rainfall intensity as compared with all other ensemble members. Alternatively, producing a TC of hurricane status, N6B develops a rain shield with broad coverage over Florida and a western rainfall bias as opposed to all other members that have an eastern accumulation bias. N6B also causes the TC to accumulate precipitation with a higher intensity over a larger area, specifically over Southern Florida and the Everglades and centrally over a wide area around Lake Okeechobee. NY and NM simulate a rain shield of moderate coverage when compared with the original Noah and N6B runs, probably due to the weaker intensity forecasts. In addition, NM accumulations consistently follow slightly to the east of the forecast storm track for the entire period. This feature in the NM rainfall pattern is also displayed in plots of the rainfall rates and rate differences between the Noah ensemble members (not shown). The NY rain also follows this pattern in the rainfall rates, yet is not pronounced in the NY rainfall accumulations. Of note are the peak rainfall accumulations in the N6B and NM members that show accumulations between 400 and 500 mm directly to the west, and between 300 and 400 mm to the north east of Lake Okeechobee. In addition, the rain rate differences of the ensemble members (not shown) reveal that the NY (NM) over (under) predicts areas of rainfall by 20–40 mm directly to the north and south of Lake Okeechobee. Thus, the impacts of the initial conditions and PBL scheme choice provide an equally strong influence on the rain field as the choice of land surface parameterization scheme.

3.5 Noah LSM water budget

So far, study results have presented changes to what the land surface is experiencing due to land experiments and the evolution of variables affecting TC intensity. This section however, examines a simulated water budget and in doing so changes the study focus from the local land scale to storm scale, specifically near the TC eye and eyewall within a radius of 270 km. A simple water budget for Fay is investigated to learn more about how the moisture is being used inside the TC and its distribution inside the system. In addition, budget terms are separated into radial and vertical components in an attempt to isolate possible moisture contributions from the storm circulation and land surface respectfully. While numerous studies were fortunate enough to observe the wind fields and develop momentum, heat and moisture budgets for specific TC cases (e.g., Gamache et al. 1993; Marks and Houze 1987; McBride 1981) and model simulations for TCs (e.g., Kurihara and Tuleya 1981; Estoque 1962) the studies of Gamache et al. (1993) and Marks and Houze (1987) resulted in a schematic of a hurricane water budget (see Fig. 1 from Gamache et al. (1993), Figs. 8a,b and 9 from Marks and Houze (1987) while Braun (2006) presents a more recent review of past observed and simulated water budget studies.

Similar to Gamache et al. (1993), this water budget calculates budget terms over a cylindrical volume taken within 270 km from the center of the TC. The model output is transformed to cylindrical polar height coordinate system following Gopalakrishnan et al. (2011), refer to Sect. 2c from this study for more details on the HWRF cylindrical transformation. Budget terms used in this analysis are adapted from the moisture flux convergence (hereafter, MFC) formulas from Banacos and Schultz (2005) who researched the use of MFC as a diagnostic forecast tool to locate regions favorable for convective

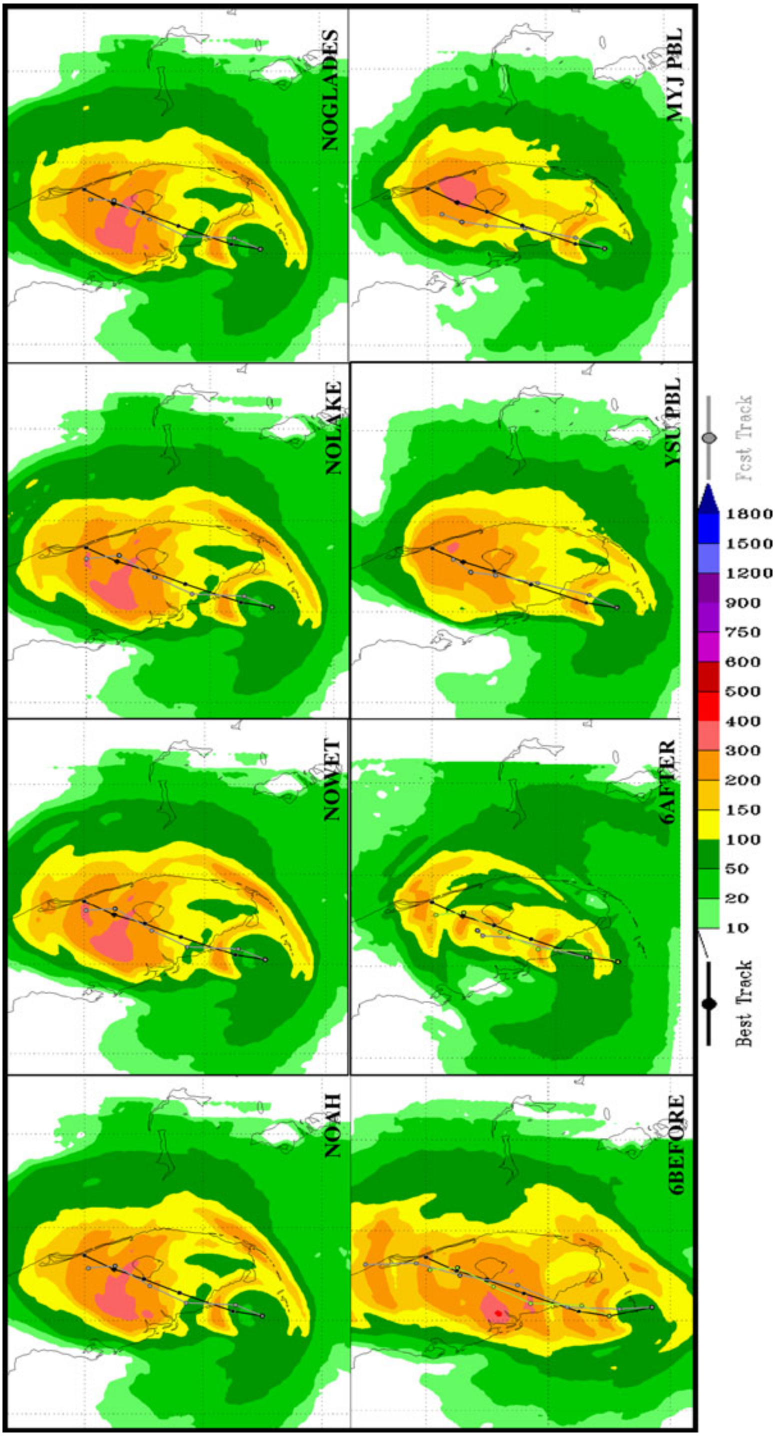

Fig. 12 Noah LSM ensemble accumulated rainfall (mm) from 00Z August 19 until 06Z August 20

initiation in the mid-latitudes (MFC was also incorporated into the Kuo cumulus parameterization for the tropics, Kuo (1965, 1974). Once the conservation of water vapor is expanded by the mass continuity equation and written in flux form for cylindrical coordinates, an analysis of the advection and convergence components of the horizontal and vertical MFC terms in the local tendency of water vapor equation is presented for TS Fay.

$$\frac{d}{dt} = \frac{\partial}{\partial t} + u_r \frac{\partial}{\partial r} + \frac{V_r}{r}\frac{\partial}{\partial \lambda} + w\frac{\partial}{\partial z} \tag{1}$$

$$\frac{dq}{dt} = \frac{\partial q}{\partial t} + \nabla \cdot (qV_h) + \frac{\partial}{\partial z}(qw) \tag{2}$$

where

$$\nabla = \hat{i}(\partial/\partial r) + \hat{j}(\partial/\partial \lambda), \quad V_h = (u_r,\ V_r/r)$$

Horizontal Advection Term (A)	$-u\frac{\partial q}{\partial r} - \frac{V_r \partial q}{r\,\partial \lambda}$
Horizontal Convergence Term (C)	$-q\left(\frac{\partial u}{\partial r} + \frac{\partial V_r/r}{\partial \lambda}\right)$
Vertical Divergence Term (D)	$+\frac{\partial}{\partial z}(qw)$
Vertical Moisture Flux (F)	$1000 \times \rho\left(\frac{\partial}{\partial z}(qw)\right)$

Within the local tendency of water vapor equation (2), terms A and C arise from the vector identity of the second term on the RHS multiplied by negative one (also known as MFC), while term D (also known as the negative vertical MFC) is the third term on the RHS of the equation. The vertical moisture in term D is investigating only the moisture that is entering the storm system as opposed to the moisture being precipitated out of the system. Generally with TC systems more moisture is being precipitated out of the system than entering the system (or study volume) so term D is considered a moisture "divergence." In the water budget analysis plots (Figs. 14, 15), a 6-hourly azimuthally averaged radius-height cross section for only the radial terms of terms A, C and terms D and F for the model vertical levels from 35 m to 15 km is used to represent the moisture distribution in conjunction with the secondary wind circulation in the TC. Results are from model simulations ALLOCEAN (NAO), Default (N) and NOOCEAN (NNO) presented at forecast hour 18, corresponding to 18Z Aug 19 which was the observed peak intensity of TS Fay.

All panels in Fig. 14 show the secondary wind circulation (uw vector field) characteristic to a TC. When comparing between simulations however, NOOCEAN has the weakest inflow and upper outflow compared to the other simulations obviously due to its weaker intensity as seen earlier in Fig. 13a,b. The moisture convergence panels (left column) each show a strongly saturated inflow layer with varying depths according to storm intensity. Notice the sloping of the moist inflow region in the ALLOCEAN and default plots. Due to the extreme amounts of moist inflow all other regions of the TC seem dry in comparison. However, warm color regions in the convergence panels are actually indicating regions of intense updrafts where moisture is being rapidly moved away from the moisture source (inflow) and seen as divergence in the figure. These updraft regions are co-located with regions of strong vertical gradients of the vertical moisture divergence (contours), the combination of these terms represent the eyewall convection. Again, the strength of the convection (shaded) and vertical gradients (contours) vary with TC intensity at 18Z Aug 19. Since Lake Okeechobee is present in both the Noah default and NOOCEAN simulations, it is possible that its presence is revealed in the panels by the second peak in vertical

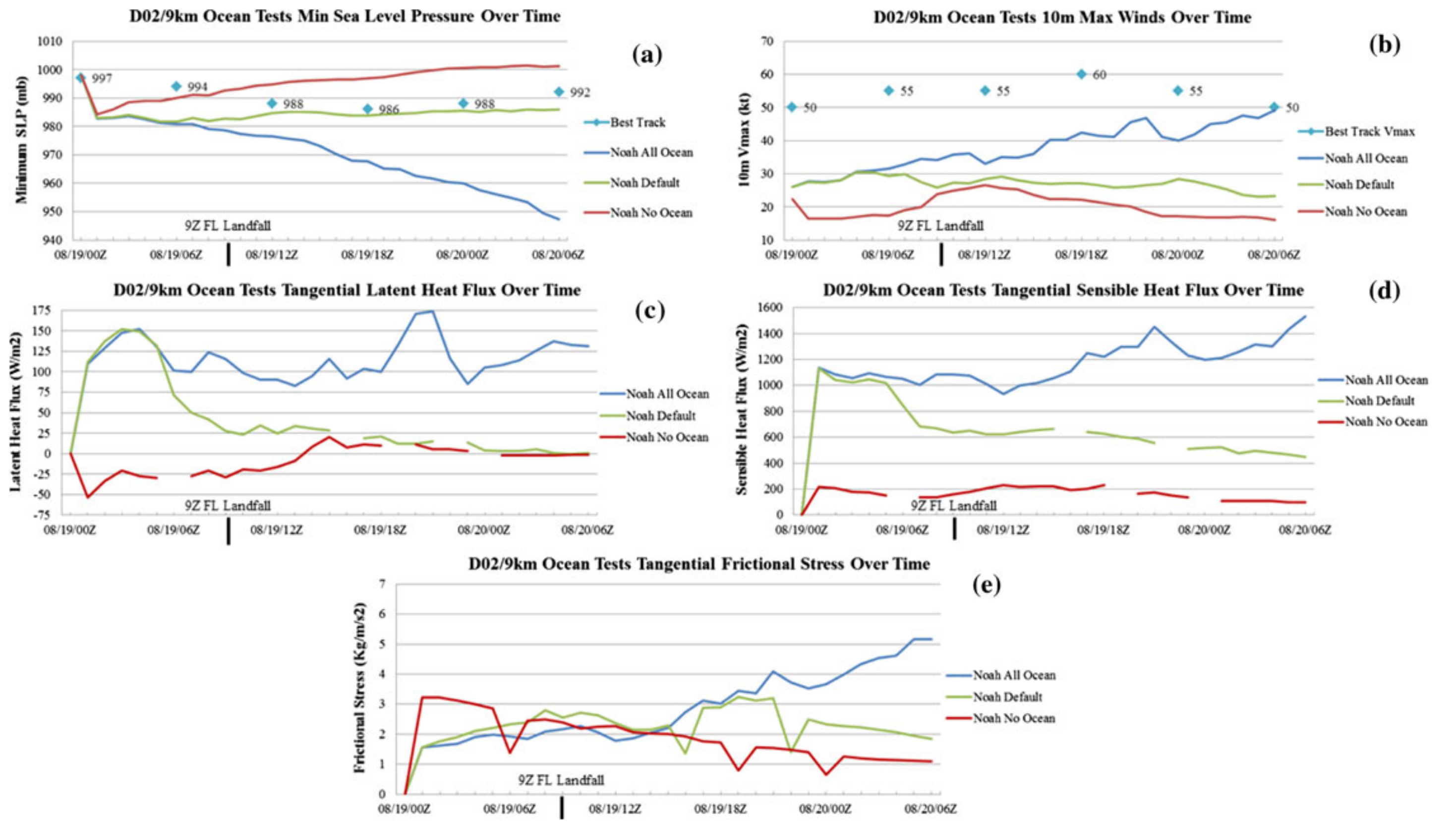

Fig. 13 Noah only ocean tests for 00Z August 19 until 06Z August 20: **a** MSLP (mb), **b** 10 m maximum winds (kt), **c** tangential latent heat flux (W/m^2), **d** tangential sensible heat flux (W/m^2), and **e** tangential frictional stress (Kg/m/s^2). Fay's Florida landfall on Cape Romano at 09Z on August 19, 2008, is indicated by the *black line*

Journal : Small 11069 Dispatch : 11-11-2011 Pages : 29
Article No. : 9841 □ LE □ TYPESET
MS Code : ☑ CP ☑ DISK

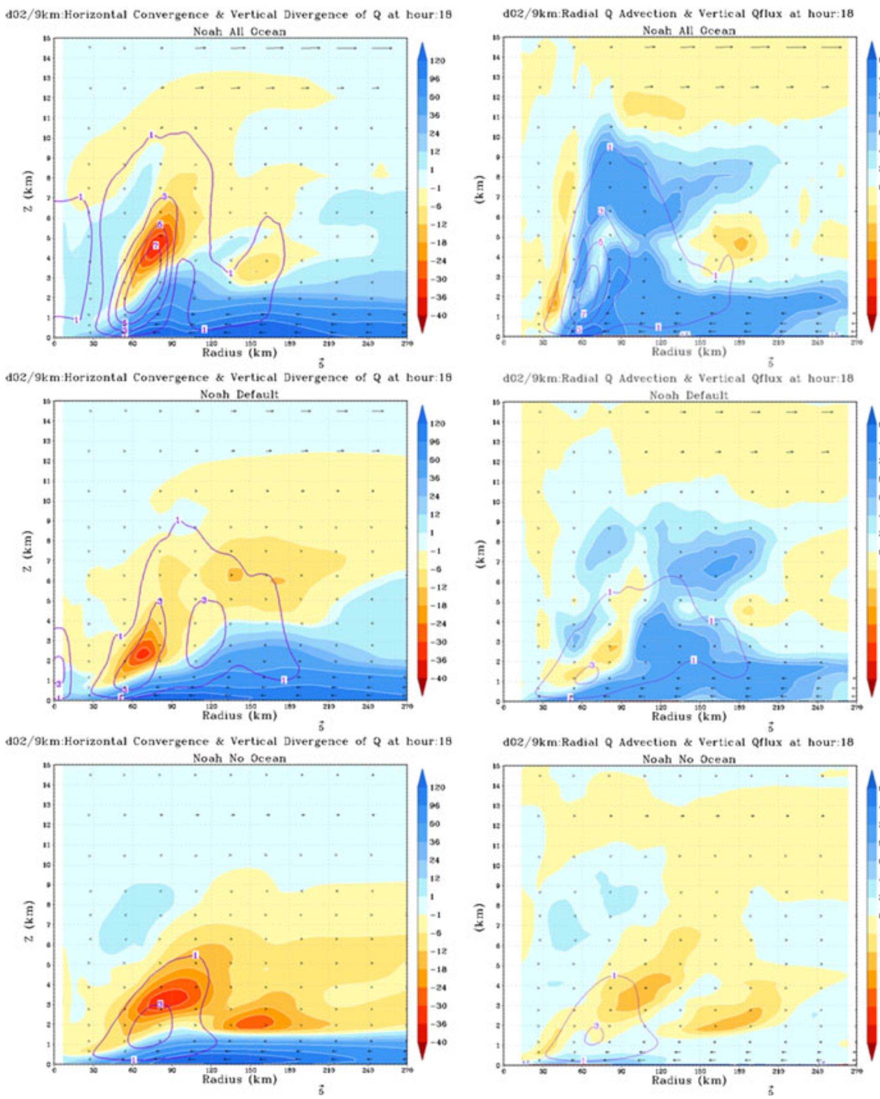

Fig. 14 Radius-height cross-section of the Noah LSM ocean tests All Ocean (*top*), Default (*middle*) and No Ocean (*bottom*) secondary circulation vectors, radial moisture convergence (kg/kg/s) with vertical moisture divergence (kg/kg*m/s, *left*) and radial moisture advection (kg/kg/s) with vertical moisture flux (g/m^{2}s, *right*) averaged over 6 hours centered at 18Z Aug 19

divergence contours in the default image and the secondary peak in convection in the shaded region slightly farther away from the TC center in the NOOCEAN image. The moisture advection panels in Fig. 14 (right column) show both how the moist inflow advection varies in intensity by the simulated storm intensity and the expansion of the moist region in the mid-levels from the eyewall throughout the mid-troposphere. The NOOCEAN simulation is unable to distribute its moisture to the mid-troposphere due to its weak intensity, however the contours of the vertical moisture in the default run seem weaker than the ALLOCEAN

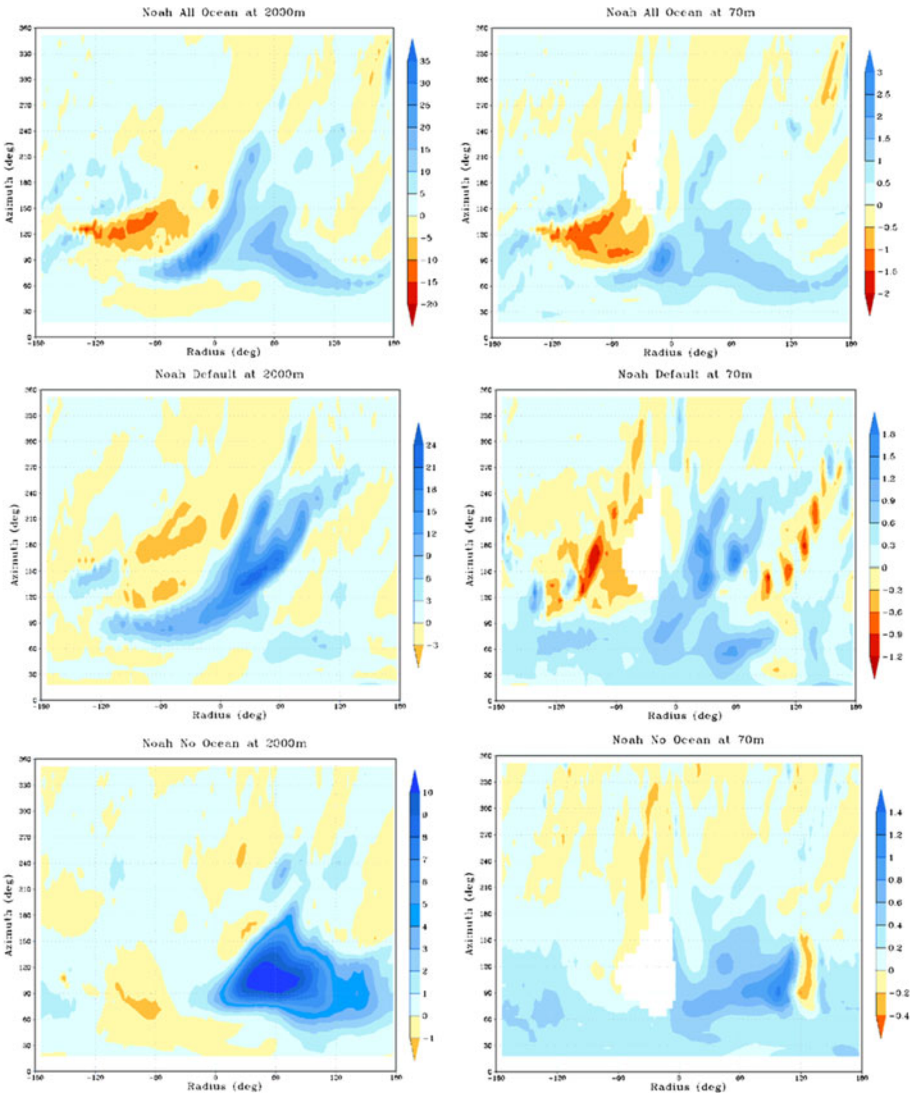

Fig. 15 Azimuth-radius horizontal plane of Noah LSM ocean tests All Ocean (*top*), Default (*middle*) and No Ocean (*bottom*) horizontal gradient of the vertical moisture flux (g/m^{2}s) at 2000 m (left) and 70 m (*right*) averaged over 6 hours centered at 18Z Aug 19

run since the default has already approached its peak state (Figs. 4a, 5a) and is now at a weakened steady state while ALLOCEAN continues to intensify with time (Fig. 13a,b). The lake moisture signature is harder to see in the radial advection panels since these images represent the horizontal advection of moisture throughout the storm as opposed to moisture being supplied vertically to the system from the surface. Therefore, the radial components are not drivers of the system but help to locate regions of convection and moisture distribution within the TC. Kuo (1974) also claimed that in TC cases the tropical cumulus convection would depend mostly on the large-scale vertically integrated MFC.

Journal : Small 11069 Dispatch : 11-11-2011 Pages : 29
Article No. : 9841 LE TYPESET
MS Code : CP DISK

Figure 15 describes the horizontal gradient of the vertical moisture flux located at the PBL top (2,000 m) and 70 m above the surface. Note the large differences in magnitude of the vertical flux between the different levels in the atmosphere; at 2000 m there are much larger values than at 70 m. The gradients of the moisture flux between ALLOCEAN and Noah default look quite similar except that the default run has a larger spatial extent of moisture flux at both levels. This feature is probably due to the presence of Lake Okeechobee. At the lower level, the region of positive moisture flux is bounded by regions of negative moisture flux which could be indicative of the lake being bounded by agricultural regions which are much drier in contrast to the lake. The moisture signature of Lake Okeechobee is most clearly seen in the NOOCEAN simulation since it is one of the only sources of moisture; this signature is especially evident at the 2,000 m level. From these results, it is conceivable to conclude that even the horizontal gradients of the vertical moisture flux assist in the sustenance of the traversing TC overland. In addition, the small gradients at the near-surface grow larger further up in the atmosphere by PBL processes as seen in the magnitude differences between the vertical levels. This conclusion agrees with statements from Banacos and Shultz (2005) that in some situations, the horizontal variations of the vertical moisture may be more important than the advective terms.

4 Conclusions

The findings of this study related to HWRF model simulations of TS Fay (2008) summarizes that three features contribute to changes in TC forecasts. First, that land surface parameterization is of importance to the storm forecast track but did not significantly impact the intensity. The improved track resulted in rainfall distributions that correctly reflect observations from hurricane studies that the core of heavy TC rain is predominantly in the narrow swath closest to the storm center (Lonfat et al. 2004; Marchok et al. 2007; Rodgers et al. 2009). In this sense, the Noah LSM seems to have better forecast performance over the GFDL Slab model. Secondly, initial boundary conditions and PBL scheme are shown to be vital to TC development and intensity forecasts of maximum winds and central pressure over land. Lastly, surface heterogeneity reflected in the land change simulations played a small but detectable role in forecast alterations. It can be seen that the presence of a lake does in fact cause a drop in central pressure of a storm, but not enough to be a major contributor to TC intensity prediction or rainfall distribution in real-world situations where an ocean basin is present.

Thus, specific to the TS Fay case, the intensification overland may have been a result of a small scale anomaly due to land surface heterogeneity and confluence caused by benevolent boundary conditions. Essentially, at the time of peak intensity, all factors acted together to produce this chance occurrence of intensification despite the known fact that TCs decay rapidly overland. The possible effects of the presence of the Florida Everglades were not important for Fay, probably mostly due to the storm track north of the Everglades. This track did not provide a substantial feedback despite the larger spatial coverage of the Everglades over Lake Okeechobee. In addition, Florida's geography may also have allowed for the ocean to continually influence the energy transport in the core of the system despite the central pressure tracking over land. Evidence of this comes from the fact that the tangential sensible heat flux curve in the Noah default member did not decrease significantly toward the extremely dry environment in the NOOCEAN case. As the latent heat flux produced expected results after landfall, in the TS Fay case perhaps the sensible heat flux was dominant in enabling the storm to strengthen over land as opposed to being greatly influenced by the inland moisture sources. From the water budget analysis, it was shown that the vertical moisture terms were more important for maintenance of Fay in the idealized simulations than the radial terms. Radial terms were essentially used to identify regions of moisture and convection, yet were not drivers for the storm. The fact that the vertical moisture terms from the budget seemed more important further agrees with the earlier finding that the fluxes are most important for sustenance of the TC. In the model framework, the combined effects of the land surface physics and initial conditions created a boundary layer feedback that seemed beneficial for the chance of Fay's intensification. The importance of this land surface feedback through the boundary layer is emphasized by the severe TC weakening resulting from the use of the two different boundary layer (YSU and MYJ) parameterizations.

A secondary result of these experiments revealed that the HWRF model is sensitive to land surface and PBL physics. In addition, we also found that it is important to have the correct initial conditions for the land surface and PBL to interact together and produce a forecast simulation that is closer to observed events. If the GFDL Slab LSM had produced a comparable track, we would have further investigated its differences from the Noah and completed a Slab water budget to see how moisture was treated using this other LSM. To further test this HWRF sensitivity, we plan to conduct this analysis on a case with longer inland track (e.g., TS Erin 2007) and a large dataset of landfalling storms in order to see if model findings from the current study are transferable to multiple HWRF forecasts of storms of varying intensities. Thus, our limitation in the current study is that it focuses on a single case, and the findings from the land cover change simulations are probably not transferable. Again, we will be investigating the predictive performance of the GFDL Slab versus the Noah LSM and testing additional physics options for supplementary analysis as needed to assist in improving the HWRF model. This larger study will include an in-depth analysis and verification of the precipitation intensity and distribution as well as a more advanced analysis of storm intensity forecasts overland.

Acknowledgments This Study benefitted in parts from the National Science Foundation CAREER grant (ATM-0847472), Department of Energy-Atmospheric Radiation Measurement (DOE ARM)-Coupled Cloud and Land Surface Interaction Campaign (CLASIC) (08ER64674) and from the National Oceanic and Atmospheric Administration (NOAA)-India Ministry of Earth Sciences (MoES) Interagency Agreement on Tropical Cyclones involving the Atlantic Oceanographic and Meteorological Laboratory (AOML), India Meteorological Department (IMD), Indian Institute of Technology (IIT) Delhi, and Purdue University.

References

Baker RD, Lynn BH, Boone A, Tao W, Simpson J (2001) The influence of soil moisture, coastline curvature, and land-breeze circulations on sea-breeze-initiated precipitation. J Hydrometeorol 2:193–211

Banacos PC, Schultz DM (2005) The use of moisture flux convergence in forecasting convective initiation: historical and operational perspectives. Weather Forecast 20:351–366

Braun SA (2006) High-resolution simulation of Hurricane Bonnie (1998). Part II: water budget. J Atmos Sci 63: 43–64

Boybeyi Z, Raman S (1992) A three-dimensional numerical sensitivity study of convection over the Florida peninsula. Bound Layer Meteorol 60:325–359

Chang H, Niyogi D, Kumar A, Kishtawal C, Dudhia J, Chen F, Mohanty UC, Sheperd M (2009) Possible relation between land surface feedback and the post-landfall structure of monsoon depression. Geophys Res Lett 36(L15826):1–6

Dastoor A, Krishnamurti TN (1991) The landfall and structure of a tropical cyclone: the sensitivity of model predictions to soil moisture parameterizations. Bound Layer Meteorol 55:345–380

Deardorff JW (1978) Efficient prediction of ground surface temperature and moisture, with inclusion of a layer of vegetation. J Geophys Res 83:1889–1903

Ek MB, Mitchell KE, Lin Y, Rodgers E, Grunmann P, Koren V, Gayno G, Tarpley JD (2003) Implementation of the Noah land surface model advances in the NCEP operational mesoscale Eta model. J Geophys Res. doi:10.1029/2002JD003296

Emmanuel KA, Callaghan J, Otto P (2008) A hypothesis for the redevelopment of warm-core cyclones over northern Australia. Mon Weather Rev 136:3863–3872

Estoque MA (1962) Vertical and radial motions in a tropical cyclone. Tellus 14(4):394–400

Ferrier BS (2005) An efficient mixed-phase cloud and precipitation scheme for use in operational NWP models. Eos Trans AGU Jt Assem Suppl 86(18):A42A–02

Gamache JF, Houze RA Jr, Marks FD Jr (1993) Dual-aircraft investigation of the inner core of Hurricane Norbert. Part III: Water budget. J Atmos Sci 50(19):3221–3243

Gopalakrishnan SG, Marks F, Qingfu L, Marchok T, Sheinin D, Surgi N, Tuleya R, Yablonsky R, Zhang X (2010) Hurricane Weather Research and Forecasting (HWRF) model scientific documentation. L Bernardet Ed 75

Gopalakrishnan SG, Zhang X, Bao J, Yeh K, Atlas R (2011) The experimental HWRF system: a study on the influence of horizontal resolution on the structure and intensity changes in tropical cyclones using an idealized framework. Mon Weather Rev 139:1762–1784

Hong S-Y, Pan H-L (1996) Nonlocal boundary layer vertical diffusion in a medium-range forecast model. Mon Weather Rev 124:2322–2339

Hong S-Y, Pan H-L (1998) Convective trigger function for a mass-flux cumulus parameterization scheme. Mon Weather Rev 129:1164–1178

Kimball S (2004) A modeling study of the sensitivity of landfalling hurricanes to surface evaporation and surface roughness. Extended Abstracts, 26th conference on hurricanes and tropical meteorology, Miami, FL, Am Meteor Soc

Kuo HL (1965) On formation and intensification of tropical cyclones through latent heat release by cumulus convection. J Atmos Sci 22:40–63

Kuo HL (1974) Further studies of the parameterization of the influence of cumulus convection on large-scale flow. J Atmos Sci 31:1232–1240

Kurihara Y, Tuleya RE (1981) A numerical simulation study on the genesis of a tropical storm. Mon Wea Rev 109:1629–1653

Lacis AA, Hansen JE (1974) A parameterization for the absorption of solar radiation in the earth's atmosphere. J Atmos Sci 31:118–133

Lonfat M, Marks FD, Chen S (2004) Precipitation distribution in tropical cyclones using the Tropical Rainfall Measuring Mission (TRMM) microwave imager: a global perspective. Mon Weather Rev 132:1645–1660

Marchok T, Rogers R, Tuleya R (2007) Validation schemes for tropical cyclone quantitative precipitation forecasts: evaluation of operational models for U.S. landfalling cases. Weather Forecast 22:726–746

Marks FD Jr, Houze RA Jr (1987) Inner core structure of Hurricane Alicia from airborne Doppler radar observations. J Atmos Sci 44(9):1296–1317

McBride JL (1981) Observational analysis of tropical cyclone formation. Part III: Budget analysis. J Atmos Sci 38:1152–1166

Moon I, Ginis I, Hara T, Thomas B (2007) Physics-based parameterization of airsea momentum flux at high wind speeds and its impact on hurricane intensity predictions. Mon Weather Rev 135:2869–2878

Pielke R (1974) A three-dimensional numerical model of the sea breezes over south Florida. Mon Weather Rev 102:115–139

Pielke RA (2001) Influence of the spatial distribution of vegetation and soils on the prediction of cumulus convective rainfall. Rev Geophys 39:151–177

Powell MD, Aberson SD (2001) Accuracy of the United States tropical cyclone landfall forecasts in the Atlantic basin (1976–2000). Bull Am Meteorol Soc 82:2749–2767

Rodgers R, Marks F, Marchok T (2009) Tropical cyclone rainfall. In: Encyclopedia of hydrological sciences, pp 1–22

Schwarzkopf MD, Fels S (1991) The simplified exchange method revisited: an accurate, rapid method for computation of infrared cooling rates and fluxes. J Geophys Res 96:9075–9096

Shen W, Ginis I, Tuleya RE (2002) A numerical investigation of land surface water on landfalling hurricanes. J Atmos Sci 59:789–802

Sousounis PJ, Fritsch JM (1994) Lake-aggregate mesoscale disturbances. Part II: a case study of the effects on the regional and synoptic-scale weather systems. Bull Am Meteorol Soc 75:1793–1811

Stuart SR, Beven JLII (2009) Tropical cyclone report, Tropical Storm Fay, 15–26 August 2008. National Hurricane Center, Miami

Journal : Small 11069 Dispatch : 11-11-2011 Pages : 29
Article No. : 9841 ☐ LE ☐ TYPESET
MS Code : ☑ CP ☑ DISK

Tuleya R (1994) Tropical storm development and decay: sensitivity to surface boundary conditions. Mon Weather Rev 122:291–304

Tuleya R, Kurihara Y (1978) A numerical simulation of the landfall of tropical cyclones. J Atmos Sci 35:242–257

Wilson JW, Megenhardt DL (1997) Thunderstorm initiation, organization, and lifetime associated with Florida boundary layer convergence lines. Mon Weather Rev 125:1507–1525